Development 133, 2705-2717 (2006) doi:10.1242/dev.02430

Analysis of mouse EphA knockins and knockouts suggests that retinal axons programme target cells to form ordered retinotopic maps

David Willshaw

I present a novel analysis of abnormal retinocollicular maps in mice in which the distribution of EphA receptors over the retina has been modified by knockin and/or knockout of these receptor types. My analysis shows that in all these cases, whereas the maps themselves are discontinuous, the graded distribution of EphA over the nasotemporal axis of the retina is recreated within the pattern of axonal terminations across rostrocaudal colliculus. This suggests that the guiding principle behind the formation of ordered maps of nerve connections between vertebrate retina and superior colliculus, or optic tectum, is that axons carrying similar amounts of Eph receptor terminate near to one another on the target structure. I show how the previously proposed marker induction model embodies this principle and predicts these results. I then describe a new version of the model in which the properties of the markers, or labels, are based on those of the Eph receptors and their associated ligands, the ephrins. I present new simulation results, showing the development of maps between two-dimensional structures, exploring the role of counter-gradients of labels across the target and confirming that the model reproduces the retinocollicular maps found in EphA knockin/knockout mice. I predict that abnormal distributions of label within the retina lead to abnormal distributions of label over the target, so that in each of the types of knockin/knockout mice analysed, there will be a different distribution of labels over the target structure. This mechanism could be responsible for the flexibility with which neurons reorganise their connections during development and the degree of precision in the final map. Activity-based mechanisms would play a role only at a later stage of development to remove the overlap between individual retinal projection fields, such as in the development of patterns of ocular dominance stripes.

KEY WORDS: Retinotopy, EphA receptors, Knockin/knockout, Induction, Quantitative model

INTRODUCTION

To establish an ordered map of vertebrate retina on superior colliculus (optic tectum in nonmammalian vertebrates), axons from retinal ganglion cells must terminate on the target structure in the correct relative positions, with the map forming in the correct orientation (Gaze, 1958; Sperry, 1963; Sakaguchi and Murphy, 1985; Stuermer, 1988). It is not known how such maps are formed, but two main classes of map-making mechanism have received particular attention (for reviews, see Goodhill and Richards, 1999; Price and Willshaw, 2000).

Activity-independent versus activity-dependent mechanisms

According to an activity-independent mechanism involving molecular recognition, each retinal ganglion cell (RGC) carries information about the position of its cell body within the retina in the form of a molecular label, and these labels are used to establish the map. Most detailed proposals of this type are based on the doctrine of chemoaffinity (Sperry, 1963), initially formulated for the retinotectal system, whereby the axon of each labelled RGC makes a connection with the tectal cell carrying the matching label. The various mechanisms proposed differ according to the ways in which they have been applied to maps obtained under normal and contrived situations, which demonstrated that retinal axons can project to areas other than those to which they project in the normal, adult projection (Gaze, 1970; Gaze and Keating, 1972; Sharma, 1972; Gaze et al., 1974; Straznicky et al., 1981).

An activity-dependent mechanism provides a way of connecting neighbouring retinal cells to neighbouring tectal cells. The general idea is that simultaneously active neighbouring cells will be more active than simultaneously active non-neighbours (Willshaw and von der Malsburg, 1976). If nerve connections are modified according to the degree of neural activity in the participating cells (Hebb, 1949), the connections between retinal neighbours and tectal neighbours will be strengthened preferentially.

One widespread view of how neural maps are formed is that an activity-independent mechanism sets up the map in sufficient precision to specify the correct polarity of the map. The detailed order within the map is then developed by means of an activity-dependent mechanism involving correlated neural activity (Fawcett and O'Leary, 1985; Schmidt and Eisele, 1985; Debski and Cline, 2002; Ruthazer and Cline, 2004). However, a lack of detailed experimental evidence has made it difficult to assess the relative importance of activity-dependent and activity-independent mechanisms. An evaluation is now possible because of the recent discovery of molecules that could act as molecular labels, coupled with the very recent findings of consistent abnormalities in retinocollicular maps in mouse formed by genetic manipulation of the putative labels (Brown et al., 2000; Feldheim et al., 2000; Reber et al., 2004).

Eph receptor tyrosine kinases are found within the ganglion cells of the vertebrate retina. Their associated ligands, the ephrins, are found in optic tectum (fish, frog and chick) and in superior colliculus (mouse) (Cheng et al., 1995; Flanagan and Vanderhaeghen, 1998). EphA receptors are distributed in a single

Institute for Adaptive and Neural Computation, School of Informatics, University of Edinburgh, 5 Forrest Hill, Edinburgh EH1 2QL, Scotland, UK.

e-mail: willshaw@inf.ed.ac.uk

Accepted 8 May 2006

continuous gradient across the nasotemporal axis of the retina; ephrinAs form a similar gradient across the rostrocaudal axis of the target (tectum or colliculus), to which the nasotemporal axis projects. Correspondingly, there is a single gradient of EphB receptor across the dorsoventral axis of the retina and a gradient of ephrinB across the mediolateral axis of the target (Hindges et al., 2002; Mann et al., 2002). In the normal map, RGCs with high levels of EphB project to target cells with high ephrinB, and RGCs with low EphB project to cells with low ephrinB. Conversely, RGCs with *high* EphA project to cells with *low* ephrinA, and vice versa. There is also evidence that ephrins are found in the retina and Ephs in the tectum or colliculus (Drescher et al., 1997; McLaughlin and O'Leary, 2005; Rashid et al., 2005).

The most quantitative characterisation of the distributions of Ephs or ephrins in the visual system has been done in the mouse. Mouse retina contains EphA4, EphA5 and EphA6 receptor types. The densities of EphA5 and EphA6 increase from nasal to temporal retina, whereas that of EphA4 remains constant. The summed density of all three receptors increases monotonically from nasal to temporal retina (Reber et al., 2004).

Scope of the paper

I present my analysis of the class of retinocollicular maps in mouse in which the normal distribution of EphA receptors within the retina has been changed by knockin and knockout manipulations (Brown et al., 2000; Reber et al., 2004). From my analysis, I propose that in the development of the ordered map, retinal axons become arranged over the colliculus according to the molecular labels (assumed to be the Eph receptors) that they carry. I show that the general form of these maps is predicted from the marker induction model (von der Malsburg and Willshaw, 1977; Willshaw and von der Malsburg, 1979).

In order to investigate how to apply this model in detail to these and related experimental findings, I developed a more specific version of the model, called the retinal induction model, in which the effects of the putative labels, Ephs and ephrins, are represented directly. I present a series of novel computer simulation results.

I present a number of predictions that can be made from the retinal induction model. These are based on the fact that, according to the model, abnormal distributions of label in the retina lead to abnormal distributions of label over the target.

MATERIALS AND METHODS

Methods for the data analysis

Insertion of EphA3 cDNA into the *Islet2* gene, contained in only 50% of the RGCs, effectively generates two populations of RGCs, one in which each cell contains the normal set of EphA receptors and one in which the cells also contain the EphA3 receptor. In these EphA3 knockin mice, the entire extent of the retina is projected in two separate ordered maps over the colliculus (Brown et al., 2000). The more rostrally located map is the projection from the EphA3$^+$ RGCs, both maps being internally ordered along the rostrocaudal dimension (Fig. 1).

The experimental data analysed here is derived from these experiments (Brown et al., 2000), together with a further set of experiments combining the knockin of the EphA3 receptor into 50% of the RGC population with the knockout of the EphA4 receptor, which affects all RGCs (Reber et al., 2004). This gives six different cases: homozygous or heterozygous EphA3 knockin without EphA4 knockout (##/++, #+/++); homozygous or heterozygous EphA3 knockin with heterozygous EphA4 knockout (##/+ –, #+/+ –); homozygous or heterozygous EphA3 knockin with homozygous EphA4 knockout (##/– –, #+/– –).

In normal retina, the distribution of total EphA receptor density across the nasotemporal axis can be described mathematically by an exponential function plus a constant (Reber et al., 2004). The same mathematical function describes the two EphA density distributions in each of the six experimental cases. The value of the constant for the EphA3$^-$ cells is different for the EphA3$^+$ cells. It also depends on which genetic manipulation was performed: the effect of EphA3 knockin is to increase the value of the constant from its normal value for the EphA3$^+$ cell population only; the effect of EphA4 knockout is to decrease its value for both populations. Changes due to a homozygous knockin or knockout are twice that for a heterozygous knockin or knockout. The relations between receptor density and distance along the nasotemporal axis for each of the six cases are given in Fig. 2, taken from Reber et al. (Reber et al., 2004).

Methods for the computational modelling

I now describe the marker induction model (von der Malsburg and Willshaw, 1977; Willshaw and von der Malsburg, 1979), which was conceived to apply to a wide range of experimental data known at the time concerned with the development and regeneration of ordered maps of connections between retina and optic tectum in non-mammalian vertebrates. Firstly I summarise the original model and then I introduce a more specific version of the model in which the properties of the Ephs and ephrins are represented directly. This new model was applied to the knockin/knockout results described here.

The marker induction model was chosen for consideration here as it is one of the few chemoaffinity-based models that proposed a specific way by which the labels would change in the experimental situations studied. It is assumed that the retinal labels are fixed and the tectal labels can change. Initially the tectal cells are unlabelled (or have weak gradients of label that are easily overwritten) and there is an initial pattern of retinotectal connections that is very diffuse. Several interlinked processes then take place to determine the final pattern of tectal labels and the final retinotectal map: (1) retinal labels are continually transferred into the tectum, through the synapses already formed, where they label the tectum (the rate of transfer into a tectal cell is determined by the total amount of retinal label present in the terminals of the axons impinging on that cell, each contribution from an individual axon being weighted by the strength of the appropriate connection); (2) tectal labels spread out into neighbouring tectal cells; (3) synaptic strengths are continually updated according to how similar the labels in the retinal cell are to the labels in the tectal cell.

By these means, the labels on each tectal cell come to resemble the labels in the cells in a small circumscribed area of retina, so defining a one-to-one mapping between retina and tectum. Introduction of an initial bias, either through the initial pattern of connectivity or through initial weak tectal labels, enables the various part-maps to be aligned in the desired orientation, resulting in an ordered map of connections. With the development of this map, a copy of the retinal labels has become *induced* into the tectum.

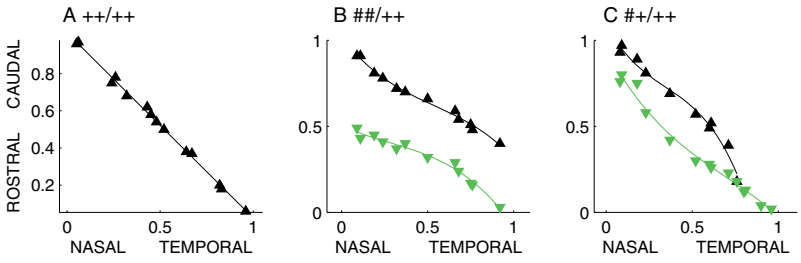

Fig. 1. The projection of nasotemporal retina onto rostrocaudal superior colliculus in EphA3 knockin mice compared with normal. (**A**) Normal; (**B**) homozygote; (**C**) heterozygote. Black-filled triangles show projections from EphA3$^-$ RGCs; green-filled inverted triangles relate to EphA3$^+$ RGCs. Redrawn from Brown et al. (Brown et al., 2000); original data kindly provided by Greg Lemke.

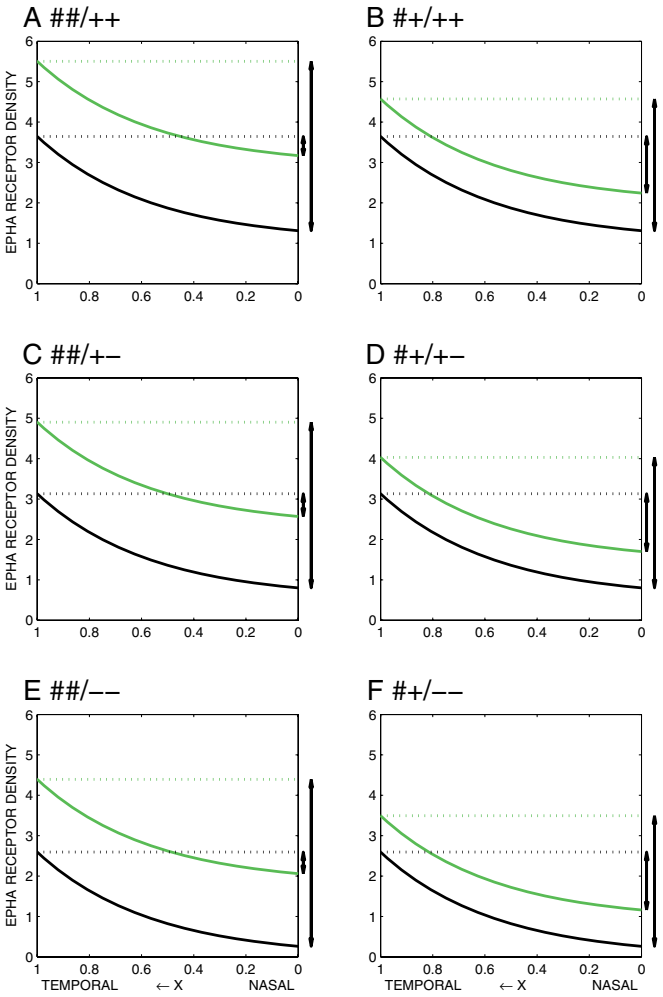

Fig. 2. How the total densities of EphA receptor in the EphA3$^+$ cells (green) and the EphA3$^-$ cells (black) vary along the nasotemporal axis of the retina, for the six experimental cases analysed. (**A**,**B**) Homozygous/heterozygous EphA3 knockin; (**C**,**D**) homozygous/heterozygous EphA3 knockin coupled with heterozygous EphA4 knockout; (**E**,**F**) homozygous/heterozygous EphA3 knockin coupled with homozygous EphA4 knockout. The two arrows at the side of each graph indicate the extent to which the range of variation in EphA density within the EphA3$^+$ population overlaps with the range of variation within the EphA3$^-$ population. The six curves are calculated from the empirical result (Reber et al., 2004) that total EphA receptor density in a RGC at a distance x along the nasotemporal axis is $0.26e^{-2.3x} + K_0$ for the EphA3$^-$ cells and $0.26e^{-2.3x} + K_0 + K_{A3}$ for the EphA3$^+$ cells. The values of the constants K_0 and K_{A3} in the six cases are: A, 1.05,1.86; B, 1.05,0.93; C, 0.54,1.77; D, 0.51,0.93; E, 0.0,1.80; F, 0.0,0.90.

The marker induction model was developed before there was any knowledge about the number or type of molecules that might function as labels. In addition, the establishment of maps between a one-dimensional retina and a one-dimensional tectum only was simulated. In order to apply the principle of induction to the knockin/knockout experiments discussed here, I have extended the marker induction model to the case of a two-dimensional array of retinal cells developing connections with a similar array of tectal (or collicular) cells as constrained by current evidence about the existence of Ephs and ephrins.

The features of this new *retinal induction model* that distinguish it from the original marker induction model are: (1) the retinal labels are assumed to be the EphA and EphB receptors, which label the nasotemporal and dorsoventral axes of the retina, respectively; (2) the tectal (collicular) labels are assumed to be the corresponding ligands, ephrinA and ephrinB, which label the rostrocaudal and mediolateral axes of the tectum or colliculus, respectively; (3) instead of regarding the retinal labels as being transported into the axonal terminals and thereby labelling the target cells, the retinal and target labels are now regarded as distinct entities, with the retinal labels within the axonal terminations upregulating the target labels; (4) in the model, the ways in which ephrinAs and ephrinBs are upregulated under the influence of EphAs and EphBs, respectively, are assumed to reflect the different ways in which the densities of EphAs and EphBs in the retina match the densities of ephrinAs and ephrinBs in the target; (5) two methods of specifying the desired polarity of the map are used, either imparting a bias to the pattern of ingrowing retinal axons or providing weak, modifiable gradients of ephrins running over the target structure; (6) a variant of the model is considered in which there is also a counter-gradient of EphA receptor running across the rostrocaudal axis of the target structure.

A schematic showing the mode of operation of the model is shown in Fig. 3. Table 1 gives the underlying mathematics.

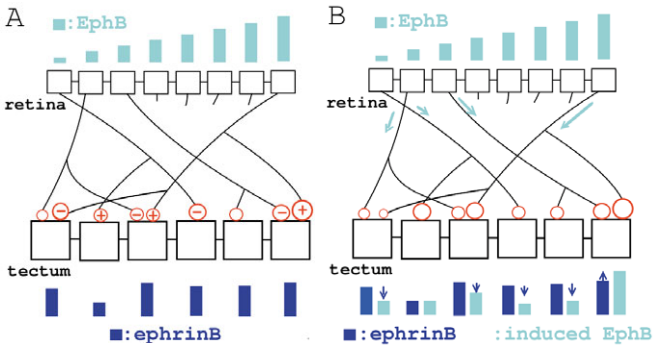

Fig. 3. Schematic of how synaptic connections and densities of ephrin in the tectum change continually according to the retinal induction model, illustrated for the EphB/ephrinB interaction. A one-dimensional retina innervates a one-dimensional tectum; not all connections are shown. (**A**) Changing the mapping. Each synaptic strength (red) is continually modified according to how closely the density of EphB (light blue) in the RGC resembles the density of ephrinB (dark blue) in the tectal cell. (**B**) Changing the tectal labels. An inductive signal is available at each tectal cell, made up from contributions from the individual axons innervating the cell. The magnitude of each contribution is in proportion to (1) the density of EphB in the parent RGC and (2) the strength of the synapse. The ephrinB density in each tectal cell is continually changed so as to reduce the difference between the current density of ephrinB (dark blue) and the density of induced EphB (light blue) at that cell. Note that the rules for the EphA/ephrinA system are more complicated: synaptic strengths are changed according to how close the *product* of the EphA density in the RGC with the ephrinA density in the tectal cell is to unity; similarly tectal ephrinA densities are changed so that the product of the induced EphA density and the actual tectal ephrinA density will tend towards unity. See Table 1 for a mathematical description of this process.

RESULTS

Results from the data analysis

The fact that abnormal distributions of EphA receptors, the putative retinal labels, produce abnormal maps (Fig. 1, Fig. 4A-F) is evidence for the involvement of the Eph receptors in map-making. Moreover, the facts that the overall map is discontinuous and that each of the two populations of RGCs makes its own ordered map support the argument that the maps formed reflect the nature of the Eph receptors carried by the RGC axons, rather than the spatial relationships among retinal cells, which would be expected in any neighbour-matching mechanism.

Table 1. Mathematical description of the retinal induction model

The model is defined by coupled sets of differential equations for how the values of the labels in the tectal cells and the strengths of the retinotectal synapses change in response to the amount of retinal labels in the axons innervating these cells.

Definitions

1. Each retinal cell i contains different amounts R_i^A and R_i^B of the molecular labels that represent the density of receptors EphA and EphB in that cell. The EphA and EphB receptor profiles are expressed as two orthogonal gradients of labels across the retina.
2. Each tectal cell j contains different amounts T_j^A and T_j^B, of the molecular labels that represent the density of ligands ephrinA and ephrinB in that cell.
3. The *synaptic strength* between retinal axon i and tectal cell j is S_{ij}.
4. The parameters α, β, γ and κ are constants.
5. The amounts of *induced label* I_j^A, I_j^B are the sums of the total density of EphA and EphB available in the terminals of the axons impinging on tectal cell j. In calculating the amounts of induced label at a given tectal cell, the contributions from the different axons are weighted by the appropriate synaptic strengths.

$$I_j^A \equiv \Sigma_k S_{kj} R_k^A / \Sigma_k S_{kj} , \quad I_j^B \equiv \Sigma_k S_{kj} R_k^B / \Sigma_k S_{kj} .$$

Labelling the tectal cells. In each tectal cell, the rate at which label is produced depends on the total amount of induced label. The density T_j^A of ephrinA in cell j changes until the product of T_j^A with the amount of induced label I_j^A attains a constant value (here set at 1), subject to a condition enforcing spatial continuity through short range interchange of label between cells

$$\Delta T_j^A = \alpha(1 - I_j^A T_j^A) + \beta \nabla_m^2 T_j^A , \quad (1)$$

where the Laplacian operator ∇_m^2 is calculated over the m nearest neighbours of cell j.

The amount T_j^B of label B in cell j is changed until it is identical to the induced label I_j^B.

$$\Delta T_j^A = \alpha(I_j^B - T_j^B) + \beta \nabla_m^2 T_j^B . \quad (2)$$

Determining the synaptic strengths. The strength of each synapse is set according to the similarity between the labels carried by the retinal cell and the tectal cell concerned. For any synapse (i,j), the closer the product of R_i^A with T_j^A is to the preset level of 1 and the closer the amount of R_i^B approaches that of T_j^B, the higher the similarity. Competition is introduced by normalising the total synaptic strength from each retinal cell to 1; a synaptic strength can be interpreted as the probability of a given retinal axon contacting a given tectal cell.

To calculate a measure of similarity, Φ, between the labels in retinal cell i and those in tectal cell j, first define the distance measure Ψ

$$\Psi_{ij} \equiv (R_i^A T_j^A - 1)^2 + (R_i^B - T_j^B)^2 .$$

Then define Φ as

$$\Phi_{ij} \equiv exp(-\Psi_{ij}/2\kappa^2) .$$

The change in synaptic strength ΔS_{ij} is

$$\Delta S_{ij} = (S_{ij} + \gamma \Phi_{ij}) / \Sigma_k (S_{ik} + \gamma \Phi_{ik}) - S_{ij} . \quad (3)$$

The computer program for solving Equations 1, 2 and 3 numerically was written in MATLAB. α=0.05, β=0.01, γ=0.1, κ=0.72; in the simulations for Fig. 6, γ was set at 0.01.

There are marked differences between the maps from homozygous and heterozygous knockins (Reber et al., 2004). In the homozygous knockin, the two maps are clearly separate and each occupies approximately half of the rostrocaudal extent of the colliculus (Fig. 4A,C,E). In the heterozygous knockin, the two maps can occupy different unequal extents of the colliculus and tend to coalesce in rostral colliculus, temporal RGCs projecting to a single area of colliculus (Fig. 4B,D,F).

These differences can be related to the degree of overlap between the range of variation of EphA density within the EphA3$^-$ population of RGCs compared with the range within the EphA3$^+$ population. As shown in Fig. 2, the overlap for the homozygous knockins is very much less than that for the heterozygous knockins. This suggests that the precise form of these discontinuous maps can be understood by studying the details of the distributions of EphA over the two populations of retinal cells, for each of the experimental cases.

I follow Brown and co-workers (Brown et al., 2000) in assuming that the value of the label of a collicular cell is determined by its total EphA density. I used the relation between EphA receptor density and retinal position (Reber et al., 2004) to construct maps of receptor density, rather than retinal position, in the axons projecting to the colliculus. Fig. 5A-F shows that the graded variation in total EphA density across the RGCs is recreated within the pattern of terminations of these cells across the superior colliculus. Regardless of the actual numerical values of EphA receptor density of individual axons, axons with greatest EphA density project rostrally and those with least density project caudally. This result, seen in all six experimental cases, suggests strongly that the mechanism that arranges the projection of RGCs from across the nasotemporal extent of the retina onto positions across the rostrocaudal axis of the colliculus involves a sorting out of retinal axons according to the amount of label, in the form of the density of EphA in their axons that they carry.

Results from the computational modelling

First of all I illustrate the properties of the retinal induction model using computer simulation results. I then go on to apply the model to the series of EphA knockin/knockout results discussed here.

The normal map

Map polarity specified by incoming fibres

I had to check whether in the model one label type per spatial dimension is sufficient to develop maps between two-dimensional structures, especially when the EphA and the EphB receptors upregulate the ephrinAs and the ephrinBs in different ways. Fig. 6 shows the simulated development of retinotectal connections in *Xenopus laevis* (Gaze et al., 1974). Cells are added to the retina at the periphery and to the tectum in a rostrolateral-to-caudomedial direction, and so this example also tests the capacity for tectal cells to be relabelled in response to the addition of new cells during development (Straznicky and Gaze, 1971; Straznicky and Gaze, 1972). There are no labels in the tectum initially, and the polarity of the map is determined by the very approximate order within the incoming fibres. The shift in the map over time is indicated clearly in column four of Fig. 6 by the movement of the red disc marking the projection of the oldest retinal cell. The green disc marks the projection of the most dorsotemporal retinal cell (which should project to the rostrolateral corner of the tectum), thus indicating that the desired orientation has been attained. It is also verified that modification of a single set of synapses suffices to enable a gradient of ephrinB to emerge in the tectum, which is a direct copy of the EphB gradient in the retina, while at the same time the ephrinA gradient that emerges is the inverse copy of the retinal EphA gradient.

Map polarity specified by weak pre-existing concentration gradients

I then carried out simulation experiments to investigate the development of maps when the polarity of the map is specified by initial weak gradients of ephrinA and ephrinB over the target structure

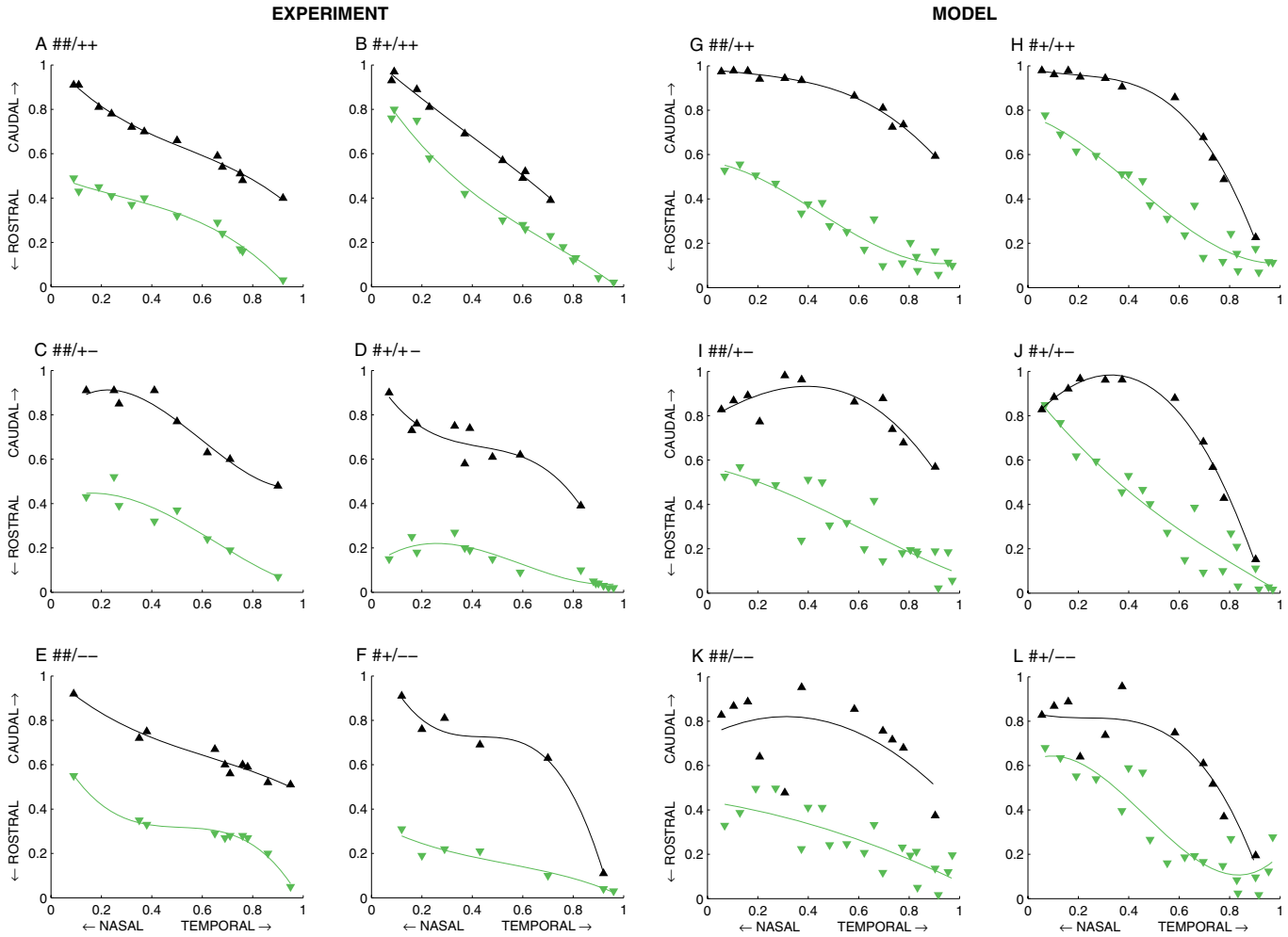

Fig. 4. The mapping of the nasotemporal axis of mouse retina onto the rostrocaudal axis of the colliculus. (**A-F**) The six experimental cases investigated by Reber and co-workers (Reber et al., 2004). Green-filled inverted triangles are projection points from EphA3^{+} cells; black-filled triangles are points from EphA3^{-} cells. Cubic fits to the data are shown. Data values kindly provided by Greg Lemke. (**G-L**) The plots obtained from computer simulations of the retinal induction model, assuming EphA distributions in the retina as given in Fig. 2; other parameter values are given in the legend to Table 1.

instead of through the initial arrangement of retinal fibres arriving at the target. I studied the development of maps between a full-size simulated retina and a full-size simulated tectum or colliculus. As the map develops, these initial target labels are overwritten (Fig. 7A). For comparison, Fig. 7B shows the development of a disordered map in the absence of any map polarity cues, with random initial connectivity and random initial distributions of ephrins.

Counter-gradients of EphA

There is evidence that other Eph and ephrin receptors label the retina and the tectum/colliculus (Drescher et al., 1997; McLaughlin and O'Leary, 2005; Rashid et al., 2005). To demonstrate the flexibility of the model, I show how the finding that the EphA7 receptor is distributed in graded form over the rostrocaudal axis of mouse colliculus, with high EphA7 in rostral colliculus and low EphA7 in caudal colliculus (Rashid et al., 2005), can be incorporated. A basic assumption of the model is that ephrinA is upregulated by EphA in such a way that high EphA leads to low ephrinA, and vice versa. This means that the high-to-low graded distribution of EphA7 over the rostrocaudal axis of the colliculus will act so as to reinforce the low-to-high distribution of ephrinA in the same direction.

In the model, the precise effect of counter-gradients of EphA in the colliculus depends on whether the effect is temporary or permanent.

Temporary action

If the EphA7 receptors act only during the initial stages of map development, effectively the EphA7-derived ephrinAs will enhance the initial weak ephrin gradients. We can then regard the polarity of the map as being specified partly by the initial ephrinA gradient and partly by the initial EphA7 gradient. Removal of the EphA7 contribution makes the map polarity cues weaker, which can result in distortions to the map or a lack of map alignment in the correct direction. As the cues get weaker, the map gets more disorganised; the extreme case of no polarity cues is shown in Fig. 7B.

Permanent action

One way in which the EphA7 gradient can have an ongoing effect throughout development is to regard the supply of available EphA7 as an extra input to each collicular cell, in addition to the supply provided in the incoming retinal fibres (Fig. 8A). It is as though, throughout development, the label supplied to each collicular cell

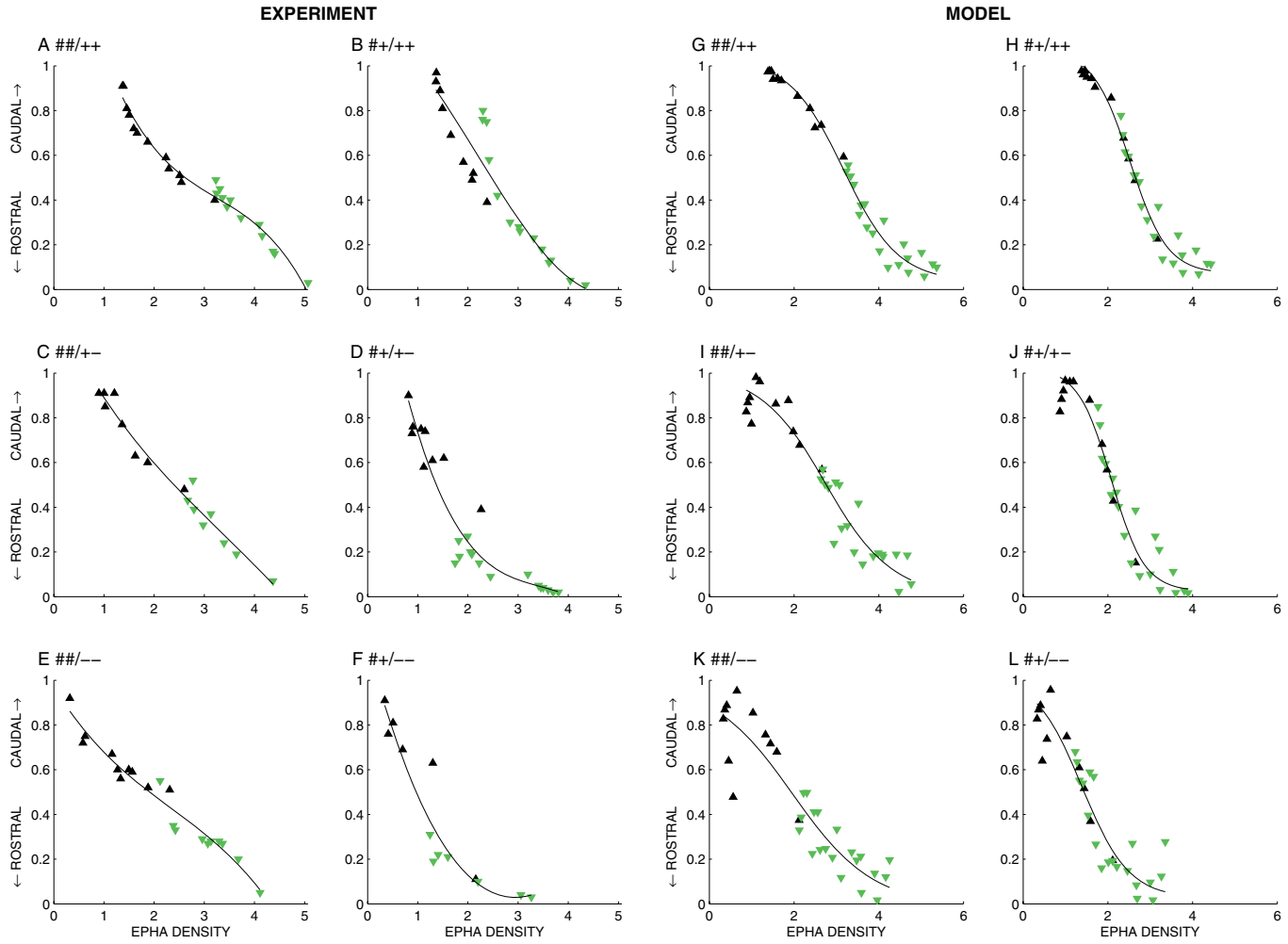

Fig. 5. The density of EphA receptor in the axons innervating a particular collicular location, for the six cases considered. (**A-F**) Plots of the experimental data shown in Fig. 4A-F after converting retinal position into EphA receptor density using the empirical relationships given in Fig. 2. (**G-L**) Plots obtained from the simulation data shown in Fig. 4G-L in a similar way. The black lines show cubic fits to the data.

has a fixed, as well as a variable, component. Removal of the EphA7 gradient (or weakening the input from the retinal fibres) can lead to distortions in the map, as when a temporary action is assumed; enhancement of the EphA7 gradient can lead to a systematic distortion of the map once the fixed component of the collicular label predominates (Fig. 8B).

These results illustrate how counter-gradients in the colliculus can be represented in the model. Use of the model permits the consequences of specific hypotheses about the role of such gradients to be worked out. Different types of connectivity pattern arise depending on the mode of interaction assumed at the cellular level. Further experimental work would be helpful in tying down further the roles of the various gradients involved.

Map precision

To provide quantitative measures for the precision of the map, it was necessary to calculate two quantities: the mean receptive field size of individual collicular cells (*field size*) and the mean separation of receptive field centres (*field separation*) from neighbouring collicular cells. To attain ordered maps, both measures must be at least as small as the mean distance between neighbouring RGCs. In the development of ordered maps (Fig. 7A, Fig. 8A), field separation decreases quickly (Fig. 9A,C), but it is not until field size also reduces to a near optimal figure that the maps become ordered; in the development of the disordered map (Fig. 7B), the projection shrinks rapidly then expands as both measures re-attain their initial high level (Fig. 9B); for the partially ordered map (Fig. 8B), the receptive fields stay high, whereas the field separation decreases, staying significantly larger than the optimal (Fig. 9D).

These results confirm that the maps reach a stable state and that the precision attained in the ordered map is not far short of the optimum. Note that there is still substantial overlap in the receptive field or, equivalently, a substantial overlap of retinal arborisation on the colliculus. The limit of precision in the map is controlled by the sensitivity of cells to respond to small fluctuations in Eph and ephrin density; increasing the numbers of cells maintains the values of these precision measures at around the mean spacing between retinal cells, thereby increasing the precision in the map.

EphA knockin/knockout maps

The qualitative model

In all maps, whether normal or abnormal, an induction model predicts that there will be a single graded distribution of ephrinA across the rostrocaudal axis of the colliculus. This is matched by a graded (but inverted) distribution of EphA receptors in the axonal terminals along this axis of the colliculus (Fig. 10). In normal

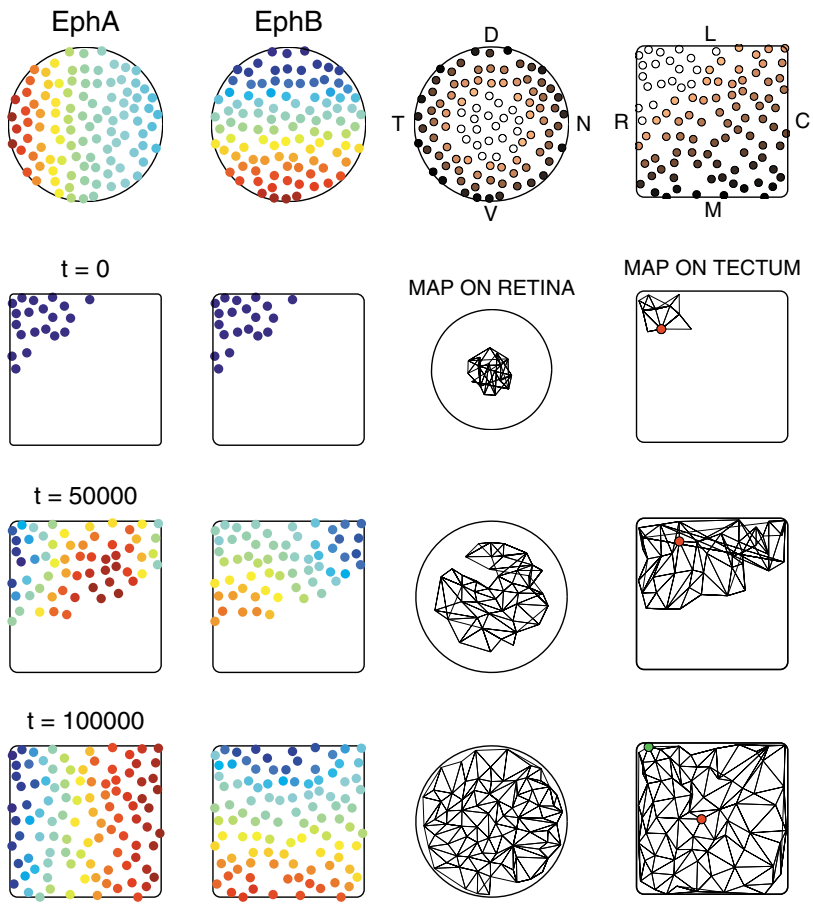

Fig. 6. The development of the *Xenopus* retinotectal map according to the retinal induction model. Twenty cells are added to both retina and tectum at timesteps 0, 20000, 35000, 55000 and 80000. Each newly arriving axon makes its initial contacts at random within a 90° arc, centred at the retinotopically appropriate tectal position available to it. Top row. To the left are the colour-coded distributions of EphA and EphB over the retina. Different colour scales are used for EphA and EphB. To the right are shown the location of individual cells within the retina (circle) and within the tectum (square). The shading indicates the growth of the retina, from centre to periphery, and of the tectum, from rostrolateral to caudomedial. The required orientation of the map is that temporal (T), nasal (N), dorsal (D) and ventral (V) retina projects to rostral (R), caudal (C), lateral (L) and medial (M) tectum, respectively. Second row. The initial mapping. The two plots to the left show the distribution of the reciprocal of ephrinA density and the actual ephrinB density over the population of tectal cells existing at that time. Plotting the reciprocal of the ephrinA density eases the comparison between the distribution of EphA over the retina and that of ephrinA over the tectum. The two plots to the right show the initial map of tectum projected onto the retina through the connections made and the same information shown as a map of retina onto tectum. Each node of the lattice comprising the map of tectum onto retina marks the retinal location eliciting maximal response from a different tectal cell; each link connects the retinal positions associated with neighbouring tectal cells; similarly for the map of retina onto tectum. Third row. Similar plots at an intermediate stage in development. Bottom row. The final mapping. In the retinotectal maps, the projection from the oldest retinal cell, from central retina, is marked by a red disc and that of the most dorsotemporal retinal cell (which should project rostrolaterally) by a green disc. The distribution of EphA density over the nasotemporal retina is as given for wild-type retina in the legend to Fig. 2; EphB density along the dorsoventral axis is assumed to vary linearly.

animals, this distribution of receptor in the terminals of the axons spreads over the colliculus matches a similar graded distribution of EphA receptors in the RGCs along the nasotemporal axis of the retina, meaning that the retinotectal map is ordered. However, in knockin/knockout animals, because the EphA3 receptors are distributed across the retina as two interleaved gradients rather than as a single gradient, there will not be the same correspondence and the map so defined will be abnormal (Fig. 10B). As illustrated for the homozygous knockin map (Brown et al., 2000), the following key features are predicted: the EphA3$^+$ cells and the EphA3$^-$ cells each make their own ordered map, in the normal orientation, on distinct areas of the colliculus. The map made by the EphA3$^+$ cells is situated rostrally and the map by the EphA3$^-$ cells is situated caudally.

The quantitative model

Computer simulations of the retinal induction model for the development of the homozygous EphA3 knockin (##/++) map compared with normal are shown in Fig. 11. Cells in the retina were assigned equiprobably to the EphA3$^+$ class or the EphA3$^-$ class of cells (top left hand panel: EphA3$^+$, green; EphA3$^-$, black). The distributions of EphA density in cells as a function of nasotemporal position follow the quantitative relations given in Fig. 2. For the control (Fig. 11A), both green and black cells were labelled from the same distribution. The bottom left hand panels of Fig. 11A,B show that whereas in the normal case an ordered map results, in the experimental case the map (coloured green) made by EphA3$^+$ cells occupies rostral colliculus and has become separated out from the normal map from EphA3$^-$ cells (coloured black).

I then simulated each of the six different experimental cases that combine knockin of EphA3 with knockout of EphA4, labelling the retina using the appropriate functions describing EphA receptor density of the retina given in Fig. 2. The plots of the one-dimensional projection of nasotemporal retina to rostrocaudal colliculus (Fig. 4G-L) reproduce the salient features of the maps shown in Fig. 4A-F. There are two separate maps across the tectum, the population of EphA3$^+$ cells projecting more rostrally. The maps are more separated for the homozygotes than for the heterozygotes. Most critically, when collicular position is plotted as a function of EphA density, in all cases there is a graded variation of EphA over the population of axons projecting from caudal to rostral extent of the colliculus (Fig. 5G-K). The main differences between the experimental and simulated connectivity plots are seen in Fig. 4D,F compared with Fig. 4J,L. These could be caused by a variety of factors, such as the nature and extent of the interactions within the colliculus assumed in the model or the relatively small number of retinal and collicular cells simulated; from the experimental side, it is not known how many RGCs are EphA3$^+$ compared with EphA3$^-$, and there is an imprecision in the labelling of retinal fibres when constructing the connectivity map.

DISCUSSION

An original analysis of the knockin/knockout series

I have analysed the maps produced in the six different types of EphA receptor knockin/knockout mice (Brown et al., 2000; Reber et al., 2004). I have shown that whereas in each case the overall map is discontinuous and apparently without a meaningful pattern, the distribution of EphA receptors within the retinal axons distributed across the rostrocaudal axis of the colliculus forms a single monotonically rising profile. This pattern is independent of the actual maximum and minimum densities of EphA receptor within the population of axons, which vary between the different experimental cases. Given that in normal maps there is an ordered projection of the nasotemporal axis of the retina onto the rostrocaudal axis of the colliculus (Simon and O'Leary, 1992), a similar gradient of EphA among the axons innervating the colliculus occurs there too.

This analysis suggests the following principle. To establish the projection of nasotemporal retina onto rostrocaudal colliculus, the axons from RGCs arrange themselves across the colliculus according to the labels that they carry. Axons with the greatest EphA density project to rostral colliculus and those with the least density to caudal colliculus. Generalisation of this principle to the sorting out of fibres along the mediolateral axis of the target as well, using the EphB receptor, gives rise to a robust strategy for map-making. The same principle will also account for a variety of retinotectal and retinocollicular maps, including the development of normal maps, the regeneration of normal maps or part-maps following surgical ablation of tissue.

The role played by retinal labels

These findings of the functional importance of retinal labels is supported by a vast amount of older, indirect, evidence from the projections formed by various types of so-called compound eyes in *Xenopus laevis*. Compound eyes are constructed by fusing together, in the embryonic eye cup, two half-eye rudiments of known origin (Gaze et al., 1963). The eye develops apparently normally, with a single optic nerve that projects to the contralateral optic tectum, but the retinotectal map is abnormal. Depending on its retinal origin,

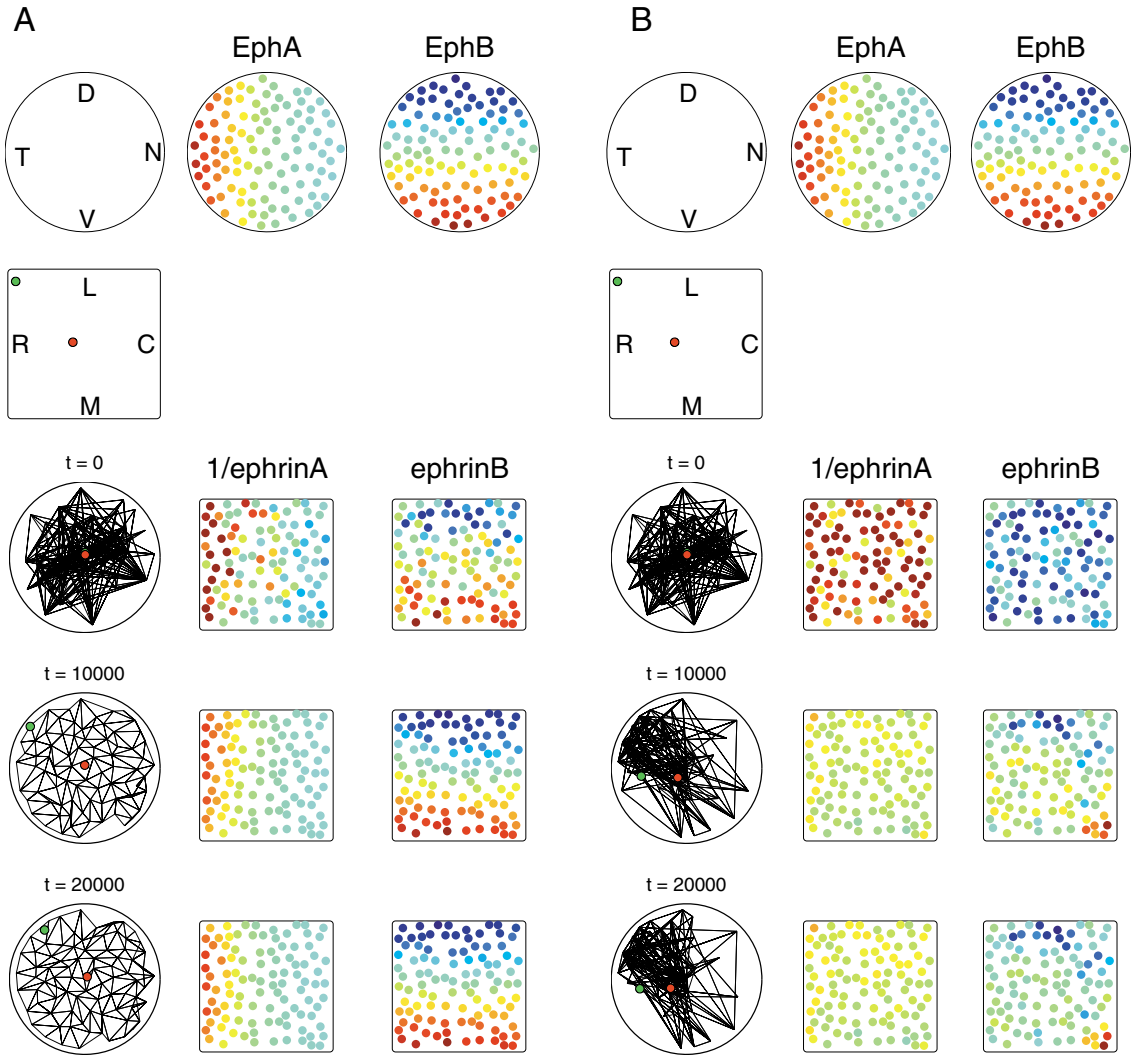

Fig. 7. Simulations of the development of connections between a full-size retina and a full-size colliculus when the initial pattern of innervation is random and the desired polarity of the map is specified by initial weak gradients of ephrins over the colliculus. (**A**) The initial concentration *C*(x) of ephrinA at a distance x along the rostrocaudal axis of the colliculus is assumed to vary as $C(x) = 0.6x + 0.5\Pi$ where Π is a random number between 0 and 1. Similarly, the initial concentration D(*y*) of ephrinB along the lateromedial axis is $D(y) = 0.6y + 0.5\Pi$. (**B**) Control with random initial ephrin distributions.

each half-eye projects on to the tectum in order and in a predictable orientation. In some cases, each of the two half-eyes projects to one half of the tectum (Gaze and Straznicky, 1980); in others, each half-eye projects to the whole of the tectum to give a double map (Gaze et al., 1963; Straznicky and Gaze, 1980; Fawcett and Willshaw, 1982). Some maps are continuous and some discontinuous (Gaze and Straznicky, 1980; Straznicky and Gaze, 1980). In all these various cases, regardless of the actual positions of the parent cells within the compound eye, axons from RGCs with the same retinal origin before transplantation to form the compound eye project to the same region of tectum, and axons of cells with different retinal origins project to spatially distinct regions of the tectum. These findings suggest strongly that the retinal cells themselves contain a memory of their original location within the eye, which is expressed in the map that they form. In other words, retinal cells carry labels that are used to form the retinotectal map and that remain fixed after surgical intervention. This conclusion is compatible with a further set of experimental findings of maps formed by pie-slice compound eyes (Willshaw et al., 1983). Here, a small portion of the retinal rudiment was replaced by a similarly sized portion from another retina that duplicated part of the host part of the compound eye. In these cases, corresponding part-duplicated maps were formed.

The analysis in the original paper describing the effects of knockin and knockout of EphA receptors on the retinocollicular map (Reber et al., 2004) concentrated on the effects of the EphA receptor, assumed to act as a retinal label. It was shown that EphA3^{+} and EphA3^{-} RGCs from the same retinal location can innervate the same region of colliculus provided that the ratio of their respective EphA densities is less than 1.36/1. It was therefore suggested that each axon can measure the ratio of the maximal EphA density in the retina compared to its own EphA density and that these normalised densities are then used as labels to determine the relative ordering of axons on the target. It was suggested that a mechanism based on that proposed by Prestige and Willshaw (Prestige and Willshaw, 1975) could act. According to

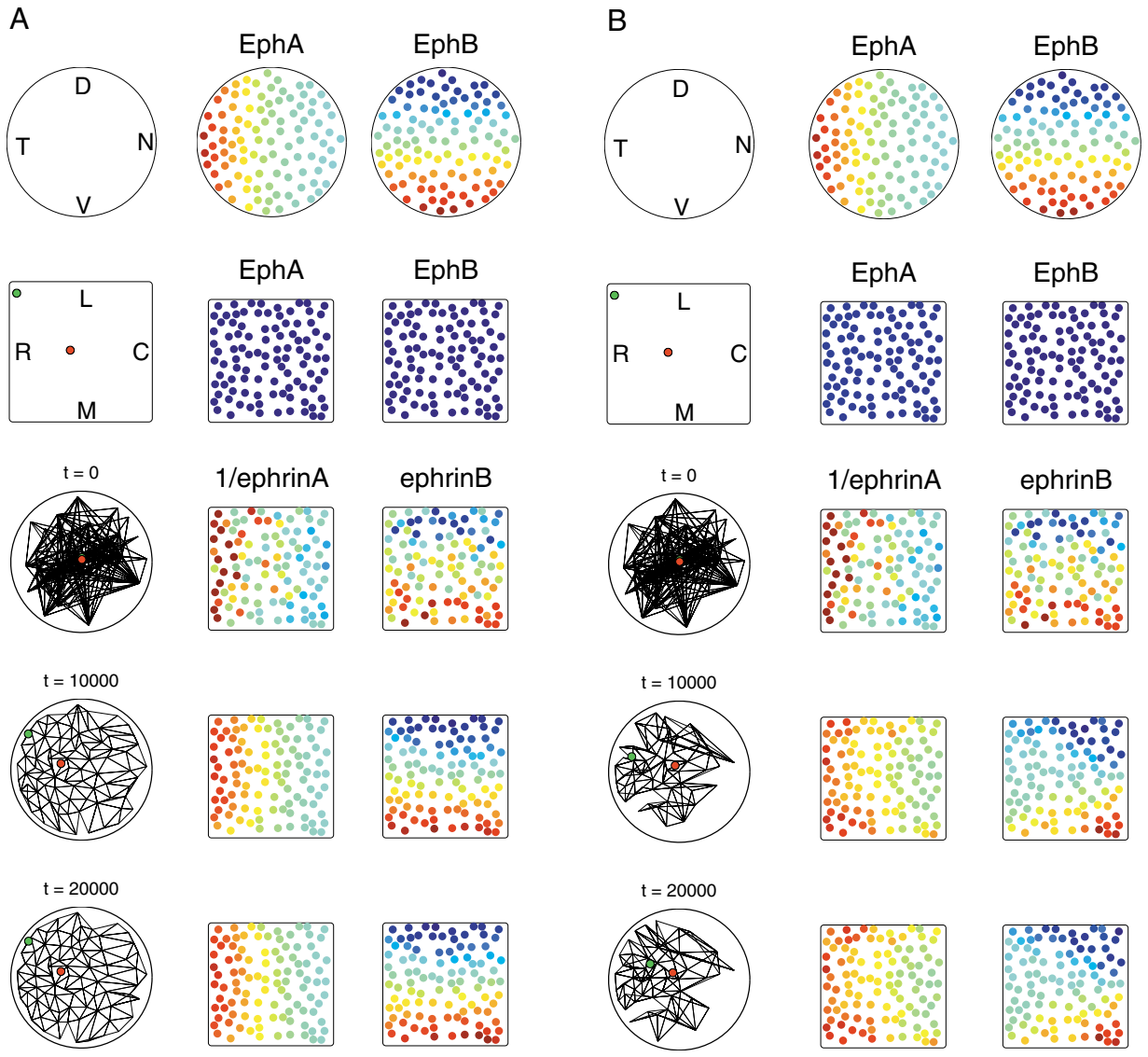

Fig. 8. The effects of introducing fixed counter-gradients of EphA over the rostrocaudal axis of the colliculus. (**A**) The simulation of Fig. 7A was repeated with a weaker initial concentration gradient over the rostrocaudal axis of 0.4x + 0.25Π together with a weak counter-gradient of EphA. The contribution from the counter-gradient is assumed to have the same functional form as the EphA gradients in the retina. At a distance x this is 0.005 + 0.013$e^{-2.3x}$ + 0.005Π. (**B**) As A but with a four times stronger counter-gradient resulting in a distorted map.

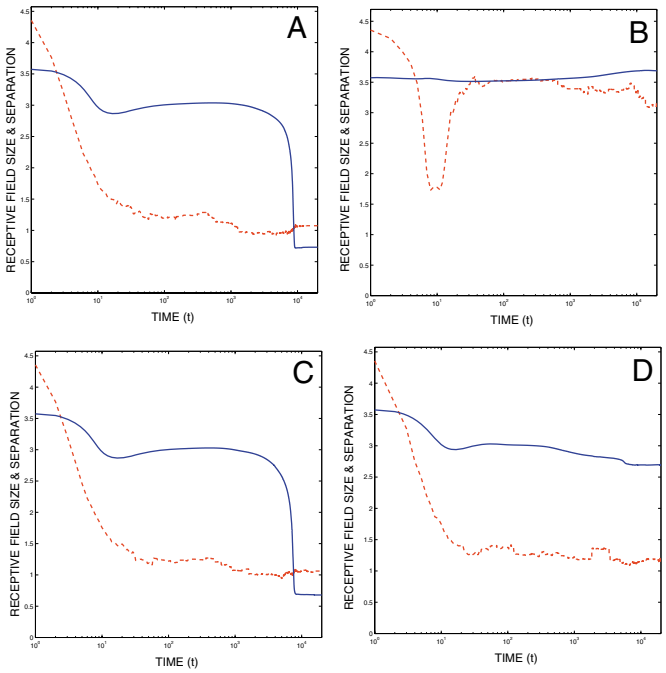

Fig. 9. How the precision of the collicular map projected on the retina changes over time for the four cases described in Figs 7, 8. The receptive field size (blue line) is the mean diameter of the receptive fields of the collicular cells; the receptive field separation (dashed line) is the mean distance between receptive field centres from neighbouring collicular cells. Both measures are expressed as ratios to the mean spacing between neighbouring retinal cells. Time plotted on a logarithmic scale. (**A**) The development of the normal map shown in Fig. 7A. Both size and separation decrease with time until they are comparable with the average spacing between retinal cells. (**B**) The development of the disordered map shown in Fig. 7B. The receptive field size stays at a high level; initially all receptive field centres congregate in one small region of the retina before they increase to give a large field separation. (**C**) The development of an ordered map with weak counter-gradients (Fig. 8A). Precision measures evolve as in A. (**D**) The development of a distorted map under the influence of strong counter-gradients (Fig. 8B). The final field size is significantly greater than in C, with the map being more disordered.

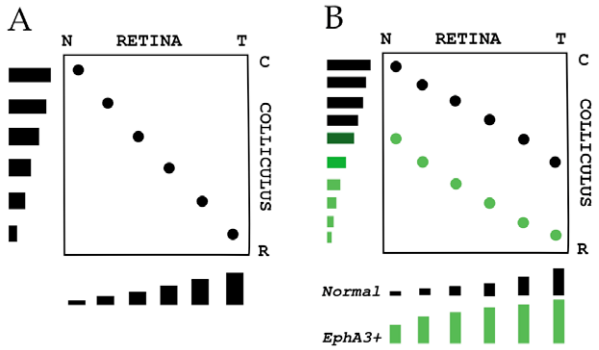

Fig. 10. Schematic of the mapping of nasotemporal retina to rostrocaudal colliculus. (**A**) Normal case. The bar chart along the horizontal axis shows the EphA receptor densities of cells positioned equidistantly along nasotemporal retina. According to an induction model, a monotonically rising profile of ephrinA is distributed across the rostrocaudal axis of the colliculus (also shown as a bar chart). The pattern of connections can be seen by finding, for each retinal cell, the collicular cells that have an ephrinA density that is the inverse of the retinal EphA density. Thus retinal cells with the largest amount of EphA connect to collicular cells with the smallest amount of ephrinA, and vice versa. (**B**) EphA3 homozygous knockin. There are two populations of retinal cells, each following a different EphA receptor density profile. Green: EphA3$^+$ cells; black: EphA3$^-$ cells. According to an induction model, the distribution of ephrinA across the colliculus will also form a monotonically rising profile, with retinal cells with the largest amount of EphA projecting to collicular cells with the smallest amount of ephrinA, and vice versa. The variation of receptor density over the retina now involves both profiles, stretching from its largest value (in EphA3$^+$ cells) to its smallest (in EphA3$^-$ cells). Because of the interleaved nature of the two overall EphA receptor density profiles in the retina, the retina will be projected twice over the colliculus, the colour coding indicating which contacts are made by the EphA3$^+$ RGCs and which by the EphA3$^-$ RGCs.

this proposal, both retinal axons and target cells are graded according to their affinities to make connections: the most affine retinal axon connects to the most affine target cell, the second-most affine axon to the second-most affine target cell, and so on. Regardless of the actual values of the affinities, an ordered map will be produced, provided that there is a limit to the number of connections that can be made, to prevent the most affine axon and target cell from dominating. As it stands, this proposal is incomplete, as in addition a mechanism is required to allow for the spreading of ordered connections seen in many experimental cases (Gaze and Keating, 1972). In addition, the question arises of why ratios have to be measured, given that the mechanism examined by Prestige and Willshaw (Prestige and Willshaw, 1975) could operate on the raw values of EphA density; a computational model would help clarify these points.

Chemoaffinity-based models for the development of retinotopic maps

Assuming that the establishment of retinotectal (or retinocollicular) maps involves the action of a set of retinal labels, what is the role of the labels in the target structure? The mechanisms that have been proposed can be classified according to whether the labels in the target are determined independently from those in the retina or whether they are dependent on the retinal labels.

Labels in the target are determined independently from those in the retina

Koulakov and Tsigankov (Koulakov and Tsigankov, 2004) developed further the arrow model (Hope et al., 1976; Overton and Arbib, 1982), according to which axons terminating near to each other on the target can swap over positions if they are the wrong way round. It was assumed (Koulakov and Tsigankov, 2004) that Eph receptors label the retina and ephrins label the target, through graded distributions of these molecules over the two structures. Axons then use knowledge of the local gradients of the distribution of label over the target to compute whether they have to interchange their positions. It was shown that both types of map seen in the EphA3 knockin experiments (Brown et al., 2000) can be generated by such a mechanism, provided that the Eph and ephrin profiles are chosen carefully.

Honda (Honda, 1998; Honda, 2003) assumed that there is a single monotonic distribution of EphA receptor across the nasotemporal axis of the retina and a similar distribution of ephrinA across the rostrocaudal axis of the colliculus. To account for the fact that high EphA maps to low ephrinA, and vice versa, it was assumed that a retinal axon seeks out and contacts with the target cell for which the product of the retinal receptor density and target ephrin density is a constant. To account for the EphA3 knockin experimental results (Brown et al., 2000), an additional mechanism allowed for repulsion

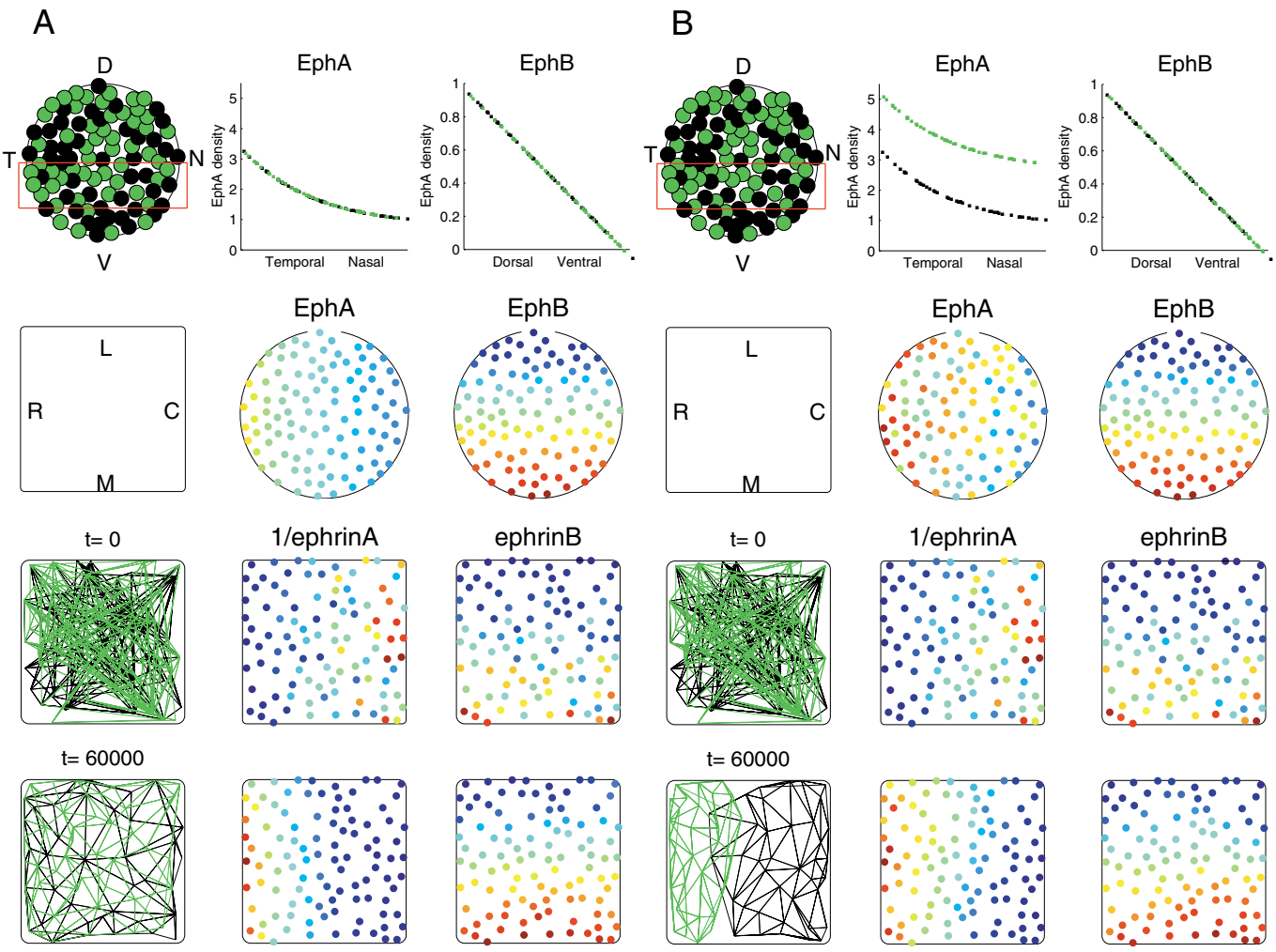

Fig. 11. Simulation of the development of the homozygous EphA3 knockin map in mouse colliculus compared to normal. The 100 retinal cells were assigned equiprobably to one of two categories, distinguished by the colours green (EphA3$^+$) and black (EphA3$^-$). The initial pattern of connectivity was random, and initially there were weak gradients of ephrinA and ephrinB over the colliculus. The maps shown are the projections from retina onto colliculus with the projections from the EphA3$^+$ and the EphA3$^-$ cells shown separately. (**A**) Control. EphA densities in EphA3$^+$ cells and the EphA3$^-$ cells are determined as for the wild-type case used in Fig. 2. A highly organised map (bottom left panel) develops from an initially disorganised state (middle left panel). (**B**) Homozygous EphA3 knockin (##/++). The EphA densities as shown in Fig. 2A were used. From the initially disorganised map, two separate ordered maps are formed (bottom row), with the green EphA3$^+$ map more rostral than the black EphA3$^-$ map. The red rectangle in the top left hand figure of A,B encloses the set of retinal cells that were used to make the one-dimensional connectivity plots shown in Fig. 4G-L.

between axons terminating in areas of the target with a high axonal density, with the result of equalising axonal density over the entire target.

Yates et al. (Yates et al., 2004) proposed a mechanism involving a combination of attraction and repulsion between axons and between target cells, coupled with a mechanism for axonal branch formation that is driven by patterned neural activity.

All three models have been applied to the homozygous and heterozygous knockin experiments reported in Brown et al. (Brown et al., 2000). As they predate the work of Reber et al. (Reber et al. 2004), they have not yet been applied to the six experimental cases described here.

Labels in the target depend on those in the retina

To my knowledge, the marker induction class of model is the only proposal in which the lability observed in the connection patterns is attributed to changes in the labels within the target structure. According to this model, once labels become assigned to the retina, they do not change as the map develops or after surgical intervention. The labels in the target (tectum or colliculus) are modifiable, by the labels carried by the retinal axons through interactions at the target.

The original papers describing the marker induction model (von der Malsburg and Willshaw, 1977; Willshaw and von der Malsburg, 1979) demonstrated how ordered maps of connections could be formed between one-dimensional structures in which a large number of molecular labels was used.

The retinal induction model embodies the marker induction model brought up to date in the light of recent biological data. Here I present several novel results.

(1) It was shown that maps of ordered connections of high precision are formed between two-dimensional structures using molecular labels with properties representing those possessed by the Ephs and the ephrins. This requires at minimum two sets of molecular types, one for each axis of the map.

(2) It was shown that ordered maps can be formed even when the mapping rules for the two molecular types are different: a gradient of ephrinB can be developed across one axis of the target structure, which matched a similar gradient of EphB across one axis of the retina, while at the same time a gradient of ephrinA, which is the inverse of the EphA retinal gradient can be developed across the other axis of the target.

(3) It was shown that the information required to specify the polarity of the map can be supplied in terms of either a bias to the initial pattern of connections or by specifying initial weak gradients of ephrins over the target structure.

(4) It was shown how the inclusion of counter-gradients of Eph receptors over the target structures affects the nature of the maps formed. Experimental data is limited here, and so the case of the counter-gradient of EphA7 was considered as a paradigm example. Different types of maps were obtained depending on whether it was assumed that these counter-gradients provide temporary or permanent guidance cues to map formation.

(5) It was shown that the marker induction model predicted the qualitative features of the EphA knockin/knockout series of experiments. In addition, detailed simulation studies of the retinal induction model reproduce the experimental results, with a high degree of correspondence between model and experiment.

Implications for future work

At the general level

Given that a mechanism involving interactions between labelled retinal axons is sufficient to form a retinotopic map, what is the role of neural activity in map-making? If electrical activity is involved, the existence of discontinuities in otherwise ordered maps, such as those seen in the EphA receptor knockin/knockout maps discussed here (Brown et al., 2000; Reber et al., 2004), and also those in several types of compound eye map (Gaze and Straznicky, 1980; Straznicky and Gaze, 1980), means that this cannot be through the use of correlated neural activity to ensure that neighbouring retinal cells connect with neighbouring cells in the target.

There is evidence that knockout of the β2 nicotinic receptor eliminates retinal electrical waves and prevents ordered retinotectal map formation (McLaughlin et al., 2003). It is possible that there is a causal link between wave activity and map formation, but currently this is unproven, as other cellular events that are more closely related to map formation may be disturbed by this knockout experiment. Much of the evidence that has accumulated for how neural activity can influence the formation of topographically ordered maps of nerve connections (Fawcett and O'Leary, 1985; Schmidt and Eisele, 1985; Debski and Cline, 2002; Ruthazer and Cline, 2004) has centred on the effects of abnormal patterns of neural activity; for example, after activity block using tetrodotoxin (Stuermer, 1990; Gnuegge et al., 2001) or NMDA receptor block using AP5 (Cline and Constantine-Paton, 1989). A parsimonious view for the involvement of neural activity is that, rather than refining an initially coarse map set up by chemoaffinity, it acts later on in development, once the precision of the map has been established. Its primary role would be to prune away the axonal arbor so as to reduce the overlap between adjacent axonal projections (Johnson et al., 1999; Ruthazer and Cline, 2004). In the special case of the double innervation of the target, in either the three-eyed frog (Constantine-Paton and Law, 1978), *Xenopus* compound eye (Fawcett and Willshaw, 1982) paradigms or by allowing optic nerve fibres to reinnervate both contralateral and ipsilateral tecta (Law and Constantine-Paton, 1980; Meyer, 1982), this will result in the formation of striped patterns of ocular dominance. On this interpretation, it would be expected that, in the three heterozygous EphA3 knockin cases discussed here, eventually discontinuous projections would develop on the rostrocaudal region of colliculus where coalescence of the projections from $EphA3^+$ cells and $EphA3^-$ cells was observed. Relevant here is that in ordered maps produced in the model (e.g. Fig. 7A), there is still substantial overlap of receptive field sizes and therefore retinal arborisations, in the final stable maps (e.g. Fig. 9A).

The specific mechanism proposed here involves the upregulation of labels in the target cells by the labels carried by the retinal axons. More direct evidence relating to this point is needed. In goldfish, upregulation of ephrins coincides with reinnervation of the optic tectum (Rodger et al., 2000), but this does not occur in frog (Bach et al., 2003).

At the specific level: the nature of the labels used

The retinal induction model has been defined in sufficient detail for the retinotectal or retinocollicular connectivity pattern to be predicted from a knowledge of a given distribution of gradients of Ephs and ephrins labelling the retina and the tectum or colliculus. This suggests new experiments and interpretations.

(1) In all contemporary models it is assumed that there are uniform distributions of cells over the retina and over the tectum or colliculus. Given data about, for example, the non-uniform distribution of RGCs in mouse (Jeon et al., 1998), it would be worth investigating the consequences of relaxing this restriction. To enable this to be done satisfactorily, additional experimental evidence is required, particularly concerning the numbers and distributions of nerve cells over the target structure.

(2) More information is needed about the properties of other molecules that could be used as labels, such as the counter-gradients of EphAs within the colliculus. In this case, the pattern of connectivity produced in the model will depend on how the molecules forming the gradients and the counter-gradients over the target interact and whether the effect of the counter-gradients is transitory or longlasting.

(3) Various experiments have demonstrated that knockout of ephrinA from the colliculus causes a lack of precision or wholesale distortions to the maps formed (Feldheim et al., 2000). This could mean that this knockout manipulation removes the machinery needed for ephrins to be upregulated under the influence of the Eph receptors in the retinal axons. In addition, or alternatively, it could be that ephrinA knockout removes the initial weak gradients over the target (Fig. 11) that determine map polarity.

(4) Assuming the EphB receptor to be the retinal label for the dorsoventral axis of the retina, knockin or knockout of members of the EphB receptor family analogous to those reported by Reber et al. (Reber et al., 2004) will result in abnormal types of maps. The precise form of these maps can be predicted from the model, once there is data about the distributions of EphB receptor over the normal retina and how these distributions are changed by the knockin/knockout manipulations.

(5) The feature of the retinal induction model that distinguishes it from all other proposals is that labels are always modifiable in the target structure, the optic tectum or the superior colliculus, and not in the retina. The most direct way of testing the model is to investigate whether the labels in the target cells are fixed or are modifiable in cases where the distribution of retinal labels is known. The obvious case to consider is that of the set of six experiments discussed here (Reber et al., 2004). The retinal induction model predicts that the distribution of label across the rostrocaudal axis of the colliculus (which is assumed here to be ephrinA) will be different

for each of the six cases analysed and will be related systematically to the distribution of EphA receptor over the population of innervating retinal ganglion cells.

The financial support of the Medical Research Council under Programme Grant PG9119632 is gratefully acknowledged. The help and advice of my colleagues, especially Stephen Eglen, Peter Kind, Peter Dayan and Geoff Goodhill, is much appreciated.

References

Bach, H., Feldheim, D. A., Flanagan, J. G. and Scalia, F. (2003). Persistence of graded EphA/ephrin-A expression in the adult frog visual system. *J. Comp. Neurobiol.* **467**, 549-565.

Brown, A., Yates, P. A., Burrola, P., Ortuno, D., Vaidya, A., Jessell, T. M., Pfaff, S. L., O'Leary, D. D. M. and Lemke, G. (2000). Topographic mapping from the retina to the midbrain is controlled by relative but not absolute levels of EphA receptor signaling. *Cell* **102**, 77-88.

Cheng, H. J., Nakamoto, M., Bergemann, A. D. and Flanagan, J. G. (1995). Complementary gradients in expression and binding of Elf-1 and Mek4 in development of the topographic retinotectal projection map. *Cell* **82**, 371-381.

Cline, H. T. and Constantine-Paton, M. (1989). NMDA receptor antagonists disrupt the retinotectal topographic map. *Neuron* **3**, 413-426.

Constantine-Paton, M. and Law, M. I. (1978). Eye-specific termination bands in tecta of three-eyed frogs. *Science* **202**, 639-641.

Debski, E. and Cline, H. (2002). Activity-dependent mapping in the retinotectal projection. *Curr. Opin. Neurobiol.* **12**, 93-99.

Drescher, U., Bonhoeffer, F. and Muller, B. (1997). The Eph family in retinal axon guidance. *Curr. Opin. Neurobiol.* **7**, 75-80.

Fawcett, J. W. and Willshaw, D. J. (1982). Compound eyes project stripes onto the optic tectum. *Nature* **296**, 350-352.

Fawcett, J. W. and O'Leary, D. D. M. (1985). The role of electrical activity in the formation of topographic maps in the nervous system. *Trends Neurosci.* **8**, 201-206.

Feldheim, D. A., Kim, Y.-I., Bergemann, A., Frisen, J., Barbacid, M. and Flanagan, J. (2000). Genetic analysis of ephrin-A2 and ephrin-A5 shows their requirement in multiple aspects of retinocollicular mapping. *Neuron* **25**, 563-574.

Flanagan, J. G. and Vanderhaeghen, P. (1998). The ephrins and Eph receptors in neural development. *Annu. Rev. Neurosci.* **21**, 309-345.

Gaze, R. M. (1958). The representation of the retina on the optic lobe of the frog. *Q. J. Exp. Physiol. Cogn. Med. Sci.* **43**, 209-224.

Gaze, R. M. (1970). *The Formation of Nerve Connections*. London: Academic Press.

Gaze, R. M. and Keating, M. J. (1972). The visual system and 'neuronal specificity'. *Nature* **237**, 375-378.

Gaze, R. M. and Straznicky, C. (1980). Stable programming for map orientation in disarranged embryonic eyes in Xenopus. *J. Embryol. Exp. Morphol.* **55**, 143-165.

Gaze, R. M., Jacobson, M. and Szekely, G. (1963). The retinotectal projection in Xenopus with compound eyes. *J. Physiol. Lond.* **165**, 384-499.

Gaze, R. M., Keating, M. J. and Chung, S. H. (1974). The evolution of the retinotectal map during development in Xenopus. *Proc. R. Soc. Lond. B Biol. Sci.* **185**, 301-330.

Gnuegge, L., Schmid, S. and Neuhauss, S. C. (2001). Analysis of the activity deprived zebrafish mutant macho reveals an essential requirement of neuronal activity for the development of a fine-grained visuotopic map. *J. Neurosci.* **21**, 3542-3548.

Goodhill, G. and Richards, L. (1999). Retinotectal maps: molecules, models and misplaced data. *Trends Neurosci.* **22**, 529-534.

Hebb, D. O. (1949). *The Organization of Behavior*. New York: Wiley.

Hindges, R., McLaughlin, T., Genoud, N., Henkemyer, M. and O'Leary, D. D. M. (2002). EphB forward signaling controls directional branch extension and arborization required for dorsal-ventral retinotopic mapping. *Neuron* **35**, 475-487.

Honda, H. (1998). Topographic mapping in the retinotectal projection by means of complementary ligand and receptor gradients: a computer simulation study. *J. Theor. Biol.* **192**, 235-246.

Honda, H. (2003). Competition for retinal ganglion axons for targets under the servomechanism model explains abnormal retinocollicular projection of Eph receptor-overexpressing or ephrin-lacking mice. *J. Neurosci.* **23**, 10368-10377.

Hope, R. A., Hammond, B. J. and Gaze, R. M. (1976). The arrow model: retinotectal specificity and map formation in the goldfish visual system. *Proc. R. Soc. Lond. B Biol. Sci.* **194**, 447-466.

Jeon, C.-J., Strettoi, E. and Masland, R. H. (1998). The major cell populations of the mouse retina. *J. Neurosci.* **18**, 8936-8946.

Johnson, F. A., Dawson, A. J. and Meyer, R. L. (1999). Activity-dependent refinement in the goldfish retinotectal system is mediated by the dynamic regulation of processes withdrawal: an in vivo imaging study. *J. Comp. Neurol.* **406**, 548-562.

Koulakov, A. A. and Tsigankov, D. N. (2004). A stochastic model for retinocollicular map development. *BMC Neurosci.* **5**, 30-46.

Law, M. I. and Constantine-Paton, M. (1980). Right and left eye bands in frogs with unilateral tectal ablations. *Proc. Natl. Acad. Sci. USA* **77**, 2314-2318.

Mann, F., Ray, S., Harris, W. A. and Holt, C. E. (2002). Topographic mapping in dorsoventral axis of the Xenopus retinotectal system depends on signaling through ephrinB ligands. *Neuron* **35**, 461-473.

McLaughlin, T. and O'Leary, D. D. M. (2005). Molecular gradients and development of retinotopic maps. *Annu. Rev. Neurosci.* **28**, 325-355.

McLaughlin, T., Torborg, C. L., Feller, M. F. and O'Leary, D. D. M. (2003). Retinotopic refinement requires spontaneous retinal waves during a critical period of development. *Neuron* **40**, 1147-1160.

Meyer, R. L. (1982). Tetrodotoxin blocks the formation of ocular dominance columns in goldfish. *Science* **218**, 589-591.

Overton, K. J. and Arbib, M. A. (1982). The extended branch-arrow model of the formation of retinotectal connections. *Biol. Cybern.* **45**, 157-175.

Prestige, M. C. and Willshaw, D. J. (1975). On a role for competition in the formation of patterned neural connexions. *Proc. R. Soc. Lond. B Biol. Sci.* **190**, 77-98.

Price, D. J. and Willshaw, D. J. (2000). *Mechanisms of Cortical Development*. Oxford: Oxford University Press.

Rashid, T., Upton, A. L., Blentic, A., Clossek, T., Knoell, B., Thompson, I. D. and Drescher, U. (2005). Opposing gradients of ephrin-As and EphA7 in the superior colliculus are essential for topographic mapping in the mammalian visual system. *Neuron* **47**, 57-69.

Reber, M., Burrola, P. and Lemke, G. (2004). A relative signalling model for the formation of a topographic neural map. *Nature* **431**, 847-853.

Rodger, J., Bartlett, C. A., Beazley, L. D. and Dunlop, S. A. (2000). Transient upregulation of the rostrocaudal gradient of ephrin-A2 in the tectum coincides with reestablishment of orderly projections during optic nerve regeneration in goldfish. *Exp. Neurol.* **155**, 196-200.

Ruthazer, E. S. and Cline, H. T. (2004). Insights into activity-dependent map formation from the retinotectal system: a middle-of-the-brain perspective. *J. Neurobiol.* **59**, 134-146.

Sakaguchi, D. S. and Murphy, R. K. (1985). Map formation in the developing Xenopus retinotectal system: an examination of ganglion cell terminal arborizations. *J. Neurosci.* **5**, 3228-3245.

Schmidt, J. T. and Eisele, L. E. (1985). Stroboscopic illumination and dark-rearing block the sharpening of the regenerated retinotectal map in goldfish. *Neuroscience* **14**, 535-546.

Sharma, S. C. (1972). The retinal projection in adult goldfish: an experimental study. *Brain Res.* **39**, 213-223.

Simon, D. K. and O'Leary, D. D. M. (1992). Development of topographic order in the mammalian retinocollicular projection. *J. Neurosci.* **12**, 1212-1232.

Sperry, R. W. (1963). Chemoaffinity in the orderly growth of nerve fiber patterns and connections. *Proc. Natl. Acad. Sci. USA* **50**, 703-710.

Straznicky, K. and Gaze, R. M. (1971). The growth of the retina in Xenopus laevis: an autodioradiographical study. *J. Embryol. Exp. Morphol.* **26**, 67-79.

Straznicky, K. and Gaze, R. M. (1972). The development of the tectum in Xenopus laevis: an autoradiographical study. *J. Embryol. Exp. Morphol.* **28**, 87-115.

Straznicky, K. and Gaze, R. M. (1980). Stable programming for map orientation in fused eye fragments in Xenopus. *J. Embryol. Exp. Morphol.* **55**, 123-142.

Straznicky, K., Gaze, R. M. and Keating, M. J. (1981). The development of the retinotectal projections from compound eyes in Xenopus. *J. Embryol. Exp. Morphol.* **58**, 79-91.

Stuermer, C. A. O. (1988). Retinotopic organization of the developing retinotectal projection in the zebrafish embryo. *J. Neurosci.* **8**, 4513-4530.

Stuermer, C. A. O. (1990). Retinotopic organization of the developing retinotectal projection in the zebrafish embryo under TTX-induced neural-impulse blockade. *J. Neurosci.* **10**, 3615-3626.

von der Malsburg, C. and Willshaw, D. J. (1977). How to label nerve cells so that they can interconnect in an ordered fashion. *Proc. Natl. Acad. Sci. USA* **74**, 5176-5178.

Willshaw, D. J. and von der Malsburg, C. (1976). How patterned neural connexions can be set up by self-organisation. *Proc. R. Soc. Lond. B Biol. Sci.* **194**, 431-445.

Willshaw, D. J. and von der Malsburg, C. (1979). A marker induction mechanism for the establishment of ordered neural mappings: its application to the retinotectal problem. *Proc. R. Soc. Lond. B Biol. Sci.* **287**, 203-234.

Willshaw, D. J., Fawcett, J. W. and Gaze, R. M. (1983). The visuotectal projections made by Xenopus 'pie slice' compound eyes. *J. Embryol. Exp. Morphol.* **74**, 29-45.

Yates, P. A., Holub, A. D., McLaughlin, T., Sejnowski, T. J. and O'Leary, D. D. M. (2004). Computational modeling of retinotopic map development to define contributions of EphA-ephrinA gradients, axon-axon interactions, and patterned activity. *J. Neurobiol.* **59**, 95-113.